



<https://tbj.ui.ac.ir>

Taxonomy and Biosystematics

E-ISSN: 3115-9001

Document Type: Research Paper

Vol. 18, Issue 3, No.68, (2026), P:29-38

Received: 13/12/2025

Accepted: 14/01/2026

Research Paper

Taxonomy of *Acantholimon* species in southern Iran: A molecular phylogenetic approach

Hossein Bibak 

Department of Plant Biology, Faculty of Biological Sciences, Tarbiat Modares University, Tehran, Iran
hbibak5878@gmail.com

Shahrokh Kazempour Osaloo * 

Department of Plant Biology, Faculty of Biological Sciences, Tarbiat Modares University, Tehran, Iran
skosaloo@modares.ac.ir

Mostafa Assadi

Botany Research Division, Agricultural Research, Education and Extension Organization (AREEO), Research Institute of Forests and Rangelands
assadi1950@yahoo.com

Abstract

Acantholimon (Plumbaginaceae) is one of the most diverse genera in Iran with 83 accepted species. Approximately 22 species are documented in the south regions of the country, 16 of which are endemic, mainly restricted to Kerman province. For this study, approximately 45 specimens were collected and analyzed to investigate taxonomic and molecular relationships. Significant taxonomic value was found in characters such as inflorescence type, flower measurements, and calyx morphology/venation. Twenty-two species (45 accessions) from four sections were analyzed using Maximum Parsimony and Bayesian methods based on nrDNA ITS and plastid rpl32-trnL_(UAG) sequences. Both datasets yielded similar, highly congruent phylogenetic trees, revealing that the *Acantholimon* sections in southern Iran are not monophyletic. Notably, the *A. scorpius* population clustered with individuals from *A. spinicalyx*, despite morphological differences. This research concludes with the development of a comprehensive diagnostic key and a species distribution map for the southern Iranian taxa. These findings establish a crucial foundation for future studies on the phylogeny, classification, identification, and conservation of the genus.

Keywords: Iran, Plumbaginaceae, *Acantholimon*, nrDNA ITS, rpl32-trnL_(UAG)

Introduction

Acantholimon Boiss. (Plumbaginaceae) is a highly diverse genus comprising approximately 321 accepted species distributed from southeastern Europe to Central Asia (POWO, 2025). It predominantly thrives in the Irano-Turanian floristic regions, particularly in Iran, Turkey, and Afghanistan (Kubitzki, 1993; Hassler, 2023; POWO, 2025). Historically, the genus *Acantholimon* in Iran has been documented to comprise 84 species according to Flora Iranica (Rechinger & Schiman-Czeika, 1974) and 79 species in the Flora of Iran (Assadi, 2005a). However, recent taxonomic work has identified several new species (Assadi, 2004; Assadi, 2005b; Assadi & Mirtadzadini, 2006; Assadi & Zeraatkar, 2020; Mahmoodi & Assadi, 2021; Bordbar & Mirtadzadini, 2022; Bibak et al., 2024). Following these latest discoveries, the recognized total number of *Acantholimon* species in Iran has consequently reached 83. The genus is predominantly found in the alpine and subalpine steppe ecosystems of the Irano-Turanian region, a unique biogeographical area defined by its arid to semi-arid climates. It has developed remarkable adaptations to survive in these harsh environments, such as xerophytic features like cushion-shaped formations and spiny leaves, which allow it to withstand drought conditions and thrive in nutrient-deficient soils (Moharrekk et al., 2019). The genus significantly contributes to soil erosion prevention due to its robust root systems and enhances

*Corresponding author

Bibak, H., Kazempour Osaloo, S. and Assadi, M. (2026). Taxonomy of *Acantholimon* species in southern Iran: A molecular phylogenetic approach. *Taxonomy and Biosystematics*, 18(3), 29-38.



3115-9001 © The Author(s). Published by University of Isfahan

This is an open access article under the CC BY-NC 4.0 License (<https://creativecommons.org/licenses/by-nc/4.0>).



<http://dx.doi.org/10.22108/tbj.2026.147757.1327>

regional biodiversity. *Acantholimon*, exhibiting an overall species endemism rate of 82% (the highest level recorded among all Iranian genera), ranks as the fourth most endemic-rich genus in Iran, with 54 endemic species (Assadi, 2006; Ghahremaninejad et al., 2025). Kerman, the central Alborz, Isfahan, and ChaharMahal-Bakhtiari provinces are among the regions in Iran with the highest levels of *Acantholimon* endemism (Khajoei Nasab & Khosravi, 2020). Approximately 22 species of *Acantholimon* have been recorded in Southern Iran, the majority of which exhibit regional endemism. Kerman Province contains the highest concentration of these endemic species within Southern Iran, accounting for 16 records. More recently, three novel species, *A. saadii* Assadi & Zeraatkar (2020), *A. assadii* Mirtadz. & Bordbar (2022), and *A. brevispicatum* Bibak, Kazempour, Assadi (2024), have been formally described from this region. Few molecular investigations have been published for the genus *Acantholimon*. Phylogenetic analyses utilizing both nuclear and plastid DNA markers consistently support close evolutionary relationships among *Acantholimon*, *Cephalorhizum* Popov & Korovin, *Limonium* Mill., *Armeria* Willd., and *Psylliostachys* (Jaub. & Spach) Nevski. Molecular data strongly suggest that *Acantholimon* is not a monophyletic genus, indicating that its current taxonomic classification is artificial (Moharrek et al., 2014; Moharrek et al., 2017). Furthermore, combined biogeographic and molecular dating analyses estimate the origin of *Acantholimon* s. l. to be in eastern Iran-Afghanistan, with subsequent diversification events spanning the Late Miocene through the Pliocene epochs (Moharrek et al., 2019). A taxonomic study of *Acantholimon* species in southern Iran was conducted, utilizing sequences from both nuclear and chloroplast genomes to assess their phylogenetic relationships. A diagnostic key and a distribution map were ultimately developed for these species.

Materials and Methods

Taxonomy study

Approximately 45 specimens of *Acantholimon* were collected during the spring and summer seasons between 2020 and 2023 from the southern region of Iran. Additionally, herbarium sheets housed at the Research Institute of Forests and Rangelands (TARI) were examined (Table 1). Specimens are also deposited in the TARI and Tarbiat Modares University Herbarium (TMUH). Morphological characters were studied both in the field and in the herbarium. The collected samples were identified using the taxonomic revision of the genus *Acantholimon* (Mobayen, 1964), Flora Iranica (Rechinger & Schiman-Czeika, 1974), and Flora of Iran (Assadi, 2005a). Data about both field observations and herbarium studies are summarized in Table 1. Distribution mapping was performed using ArcGIS version 10.6.1 (Figure 1).

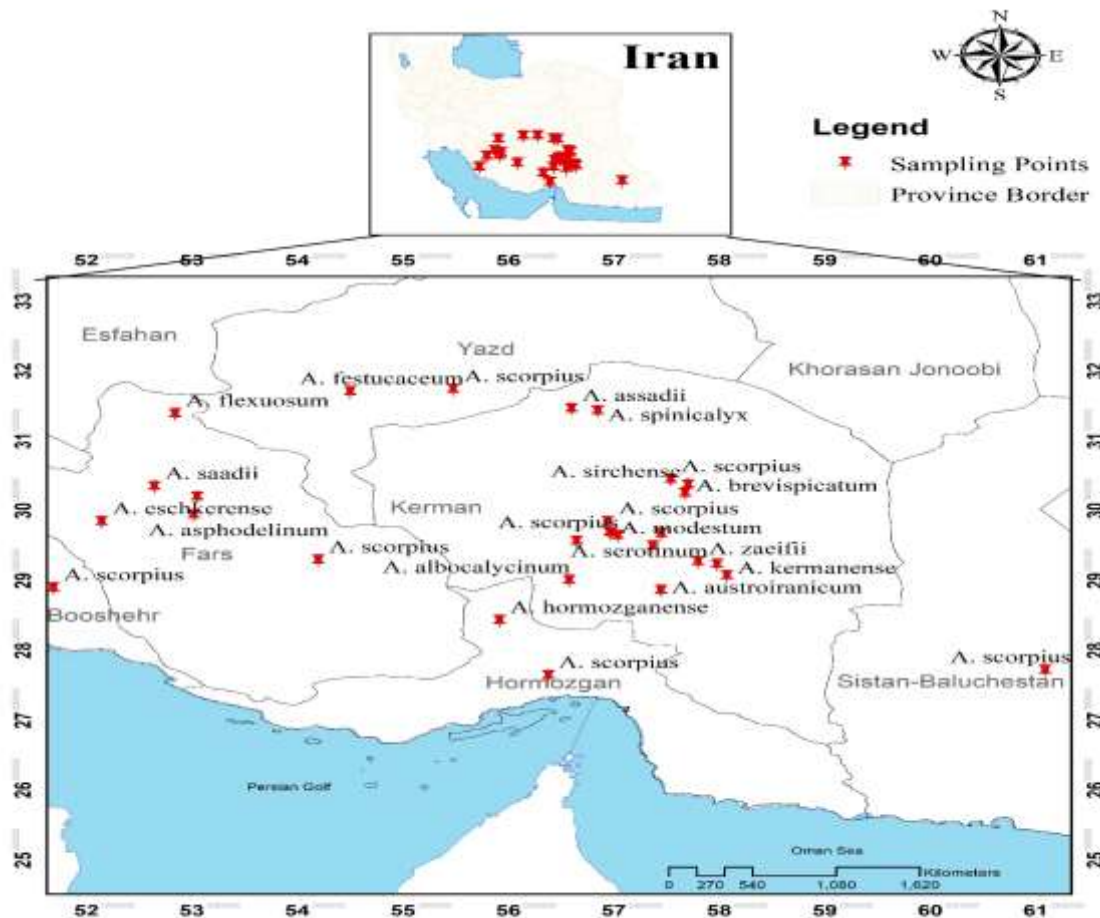


Figure 1. Distribution map of *Acantholimon* in southern Iran.
Table 1. Voucher information and GenBank accession number of examined species in molecular analysis.

Species	Voucher information	GenBank accession No. for ITS	GenBank accession No. for rpl32-trnLuAG
<i>Acantholimon albocalycinum</i> Assadi & Mirtadz. (1)	Iran: Kerman, Bibak, Tarbiat Modares University Herbarium, IRN: hb6014	PP403888	PP429322
<i>A. albocalycinum</i> Assadi & Mirtadz. (2)	Iran: Kerman, Bibak & Jarchi, Tarbiat Modares University Herbarium, IRN: hb6015	PP403889	PP429323
<i>A. asphodelinum</i> Mobayen	Iran: Fars, Jamzad et al., TARI, IRN: 69399	PP403897	PP429332
<i>A. asphodelinum</i> Mobayen	Iran: Fars, Jamzad et al., TARI, IRN: 69399	LC153812*	-----
<i>A. austroiranicum</i> Rech.f. & Schiman-Czeika	Iran: Kerman, Bibak, Tarbiat Modares University Herbarium, IRN: hb6025	PP403893	PP429327
<i>A. austroiranicum</i> Rech.f. & Schiman-Czeika	Iran: Kerman, Mirtadzadini, TARI, IRN: 83216	AB979538*	-----
<i>A. brevispicatum</i> Bibak, Kazempour & Assadi (1)	Iran: Kerman: Bibak, TARI, IRN:106850	PP403884	PP429317
<i>A. brevispicatum</i> Bibak, Kazempour & Assadi (2)	Iran: Kerman: Bibak, Tarbiat Modares University Herbarium, IRN: hb6040	PP403885	PP429318
<i>A. chlorostegium</i> Rech.f. & Schiman-Czeika	Iran: Kerman, Bibak, Tarbiat Modares University Herbarium, IRN: hb6022	PP403892	PP429326
<i>A. cupreo-olivascens</i> Rech.f. & Schiman-Czeika	Iran: Kerman, Bibak, Tarbiat Modares University Herbarium, IRN: hb6033	PP403896	PP429330
<i>A. cupreo-olivascens</i> Rech.f. & Schiman-Czeika	Iran: Kerman, Mirtadzadini, Shahid Bahonar University, IRN:1245	LC153829*	-----
<i>A. eschkerense</i> Boiss. & Hausskn.	Iran: Fars, Mozaffarian, TARI, IRN: 83648	LC153844*	-----
<i>A. festucaceum</i> (Jaub. & Spach) Boiss.	Iran: Fars, Assadi & et al, Tarbiat Modares University Herbarium, IRN: 92920	LC153852*	-----
<i>A. festucaceum</i> (Jaub. & Spach) Boiss.	Iran: Bakhteyari, Mozaffarian & et al., TARI, IRN: 57988	LC153851*	-----
<i>A. flexuosum</i> Boiss. & Hausskn. ex Bunge	Iran: Kohgiluyeh and Boyer-Ahmad, Assadi, TARI, IRN: 72426	PP403898	PP429333
<i>A. flexuosum</i> Boiss. & Hausskn. ex Bunge	Iran: Fars, Mozaffarian, TARI, IRN: 18991	AB979557*	-----
<i>A. haesarensis</i> Bornm. ex Rech.f. & Schiman-Czeika	Iran: Kerman, Bibak, Tarbiat Modares University Herbarium, IRN: hb6030	PP403895	PP429329
<i>A. hormozganense</i> Assadi	Iran: Fars, Jamzad et al., TARI, IRN:15767	LC153861*	-----
<i>A. kermanense</i> Assadi & Mirtadz.	Iran: Kerman, Mirtadzadini, Shahid Bahonar University, IRN:1242	LC153866*	-----
<i>A. kermanense</i> Assadi & Mirtadzadini	Iran: Kerman, Mirtadzadini, Shahid Bahonar University, IRN:1243	AB979566*	PP429331
<i>A. mirtadzadini</i> Assadi	Iran: Kerman, Bibak, Tarbiat Modares University Herbarium, IRN: hb6012	PP403887	PP429321
<i>A. modestum</i> Bornm. Ex Rech.f. & Schiman-Czeika	Iran: Kerman, Bibak, Tarbiat Modares University Herbarium, IRN: hb6020	PP403891	PP429325
<i>A. modestum</i> Bornm. Ex Rech.f. & Schiman-Czeika	Iran: Kerman, Mirtadzadini, Shahid Bahonar University, IRN:1244	AB979569*	-----
<i>A. scorpius</i> (Jaub. & Spach) Boiss.	Iran: Kerman, Bibak, Tarbiat Modares University Herbarium, IRN: hb6028	PP403894	PP429328
<i>A. scorpius</i> (Jaub. & Spach) Boiss.	Iran: Kerman, Bibak, Tarbiat Modares University Herbarium, IRN: hb7010	PQ577715	PQ640881
<i>A. scorpius</i> (Jaub. & Spach) Boiss.	Iran: Kerman, Bibak, Tarbiat Modares University Herbarium, IRN: hb7012	PQ577717	PQ640883
<i>A. scorpius</i> (Jaub. & Spach) Boiss.	Iran: Sistan and Baluchestan, Mozaffarian, TARI, IRN: 43911	PQ577719	PQ640910
<i>A. scorpius</i> (Jaub. & Spach) Boiss.	Iran: Sistan and Baluchestan, Mozaffarian, TARI, IRN: 42780	PQ577720	PQ640909
<i>A. scorpius</i> (Jaub. & Spach) Boiss.	Iran: Bushehr, Mozaffarian, TARI, IRN: 74072	PQ577743	PQ640906
<i>A. scorpius</i> (Jaub. & Spach) Boiss.	Iran: Bushehr, Mozaffarian, TARI, IRN: 71277	PQ577721	PQ640885

Species	Voucher information	GenBank accession No. for ITS	GenBank accession No. for rpl32-trnLuAG
<i>A. scorpius</i> (Jaub. & Spach) Boiss.	Iran: Yazd, Assadi & Bazgosha, TARI, IRN: 55996	PQ577739	PQ640903
<i>A. scorpius</i> (Jaub. & Spach) Boiss.	Iran: Hormozgan, Assadi & Sardabi, TARI, IRN: 42204	PQ577744	PQ640907
<i>A. scorpius</i> (Jaub. & Spach) Boiss.	Iran: Hormozgan Mozaffarian, TARI, IRN: 44592	PQ577733	PQ640897
<i>A. scorpius</i> (Jaub. & Spach) Boiss.	Iran: Fars, Mozaffarian, TARI, IRN: 47058	PQ577724	PQ640888
<i>A. scorpius</i> (Jaub. & Spach) Boiss.	Iran: Fars, Assadi & Sardabi, TARI, IRN: 41723	PQ577725	PQ640889
<i>A. scorpius</i> (Jaub. & Spach) Boiss.	Iran: Bushehr, Mozaffarian, TARI, IRN: 71277	PQ577721	PQ640885
<i>A. serotinum</i> Rech.f. & Schiman-Czeika	Iran: Kerman, Bibak, Tarbiat Modares University Herbarium, IRN: hb6035	PP403899	PP429334
<i>A. serotinum</i> Rech.f. & Schiman-Czeika	Iran: Kerman, Pourmirzae & Ghonchee, TARI, IRN: 83211	LC153909*	-----
<i>A. schirazianum</i> Boiss.	Iran: Fars, Dehbozorgi, TARI, IRN: 32716	LC153899*	-----
<i>A. spinicalyx</i> Kőie & Rech.fil.	Iran: Kerman, Mirtadzadini, TARI, IRN: 86985	LC154031*	LT707364*
<i>A. spinicalyx</i> Kőie & Rech.fil.	Iran: Khorasan, Mehregan, TARI, IRN: 83232	LC153913*	-----
<i>A. sirchense</i> Assadi & Mirtadz.	Iran: Kerman, Bibak, Tarbiat Modares University Herbarium, IRN: hb6017	PP403890	PP429324
<i>A. zaeifii</i> Assadi (1)	Iran: Kerman, Bibak, Tarbiat Modares University Herbarium, IRN: hb6010	PP403886	PP429319
<i>A. zaeifii</i> Assadi (2)	Iran: Kerman, Mirtadzadini, Shahid Bahonar University Herbarium, IRN: 1249	AB979587*	PP429320
<i>Psylliostachys beludshistanicus</i> Roshkova	Iran: khorassan, Faghiehnia & Zangoie, FUMH, IRN: 18122	AB979596*	PP429316

(*) nrDNA ITS sequences for those taxa were obtained from GenBank

Molecular study

The research provided new nrDNA ITS sequences for 20 species (28 accessions) and rpl32-trnL_(UAG) sequences for 17 species (31 accessions). Additionally, fifteen nrDNA ITS sequences were obtained from GenBank. Nuclear and plastid markers were combined to create a dataset for 45 taxa. Details on species, accessions, voucher information, and GenBank accession numbers are summarized in Table 1. Dried leaf samples were used to extract total genomic DNA using a modified CTAB protocol (Doyle & Doyle, 1987). The nrDNA ITS region was amplified with primers AB101F and AB102R (Douzery et al., 1999). The rpl32-trnL_(UAG) spacer was amplified with rpl32-F and trnL_(UAG)-R primers following Shaw et al. (2007). PCR amplification was performed in a microtube containing 8 µl of deionized water, 10 µl of 2× Taq DNA polymerase master mix (Red, Amplicon), 0.5 µl of each primer (at 10 pmol/µl), and 1 µl of template DNA. The nrDNA ITS region was initially predenatured at 94°C for 4 minutes. Then, 35 cycles were run: 1 minute at 94°C for denaturation, 1 minute at 55°C for primer annealing, and 90 seconds at 72°C for extension. Final extension was at 72°C for 5 minutes. The PCR protocol for the rpl32-trnL_(UAG) region included an initial predenaturation of 5 minutes at 80°C, followed by 35 cycles of 1 minute at 94°C for denaturation, 1 minute and 60 seconds at 51.5°C for primer annealing, and 60 seconds at 65°C for extension. It concluded with a 7-minute extension at 72°C. PCR products were separated on 1% agarose gels in 1x TBE buffer (pH 8) and stained with ethidium bromide. The amplified products were sequenced with appropriate primers and sent to Pishgam Inc. for Sanger sequencing. *Psylliostachys beludshistanicus* Roshkova was considered an outgroup, based on Moharrek et al. (2014, 2017).

Phylogenetic analyses

A phylogenetic study of 20 *Acantholimon* taxa was conducted using maximum likelihood (ML) and Bayesian inference (BI). The maximum likelihood analysis was performed with the W-IQ-TREE web server (Trifinopoulos et al., 2016). MrBayes version 3.2.6 (Ronquist et al., 2012) was used for the Bayesian phylogenetic analysis, which was conducted on the CIPRES Science Gateway version 3.3 (Miller et al., 2010). The best nucleotide substitution model for each locus was identified using jModelTest (Posada, 2008) based on the Akaike Information Criterion (AIC) via the Phylemon 2.0 web server (Sánchez et al., 2011), while GTR models selected by ModelFinder were applied for nrDNA data, and GTR+G models were used for plastid and combined datasets in the ML analyses.



Results

The current study's findings identify the following characters as valuable for taxonomy: inflorescence type and length; the number and length of flowers; bract shape and length; the number, size, and shape of bracteoles; calyx shape and color; calyx vein patterns; and the indumentum (or indument) of the inner calyx. Three datasets were analyzed: the nrDNA ITS sequence alignment, which included 45 accessions, spanned 622 nucleotide positions, yielding 53 parsimony-informative sites. The rpl32-trnL (UAG) matrix comprised 34 individuals, 1158 base pairs, and 67 parsimony-informative sites. Furthermore, the comprehensive combined dataset (nrDNA ITS + rpl32-trnL (UAG)) consisted of 1795 nucleotide sites, including 143 parsimony-informative sites. Detailed statistics for each dataset and their combination are presented in Table 2. For visualization, a Bayesian 50% majority-rule consensus tree was constructed, displaying both PP and BP values on the branches.

Table 2. Dataset and tree statistics from separate and combined analyses of the nuclear and chloroplast regions.

	nrDNA ITS	plastid (<i>rpl32-trnL</i> (UAG))	Combined (nr+cp)
Number of sequences	45	34	45
Nucleotide sites	622	1158	1795
Informative characters	53	67	143
Conserved sites (C)	496	949	1430
CI of MPTs	0.838	0.884	0.838
RI of MPTs	0.974	0.970	0.974
Evolutionary model selected (under AIC)	GTR	GTR+G	GTR+G

Results from the nrDNA ITS tree (Figure 2):

The tree inferred from the nrDNA ITS data resolved two major clades: Clade A and Clade B. Clade A is basal and comprises two subclades: A1 and A2. Subclade A1 included sixteen accessions: two of *Acantholimon spinicalyx* (Sect. *Tragachantina*), twelve of *A. scorpius* (Sect. *Tragachantina*), and two of *A. austro-iranicum* (Sect. *Microstegia*). Subclade A2 consisted of thirteen accessions, including *A. modestum* (2 accessions; Sect. *Tragachantina*), *A. sirschense* (1; Sect. *Glumeria*), *A. chlorostegium* (1; Sect. *Tragachantina*), *A. albocalycinum* (2; Sect. *Glumeria*), *A. haesarensense* (1; Sect. *Acantholimon*), *A. kermanense* (2; Sect. *Acantholimon*), *A. cupreo-olivascens* (2; Sect. *Glumeria*), *A. shirazianum* (1; Sect. *Microstegia*), and *A. mirtadzadinii* (1; Sect. *Acantholimon*). Clade B was resolved into two subclades: B1 and B2. Subclade B1 contained two accessions of *A. flexosum* (Sect. *Acantholimon*). Subclade B2 comprised thirteen accessions from the *Acantholimon* section: *A. festucaceum* (2), *A. zaeifii* (2), *A. flexosum* (1), *A. asphodelinum* (2), *A. serotinum* (2), *A. brevispicatum* (2), *A. hormozganense* (1), and *A. eschkerense* (1).

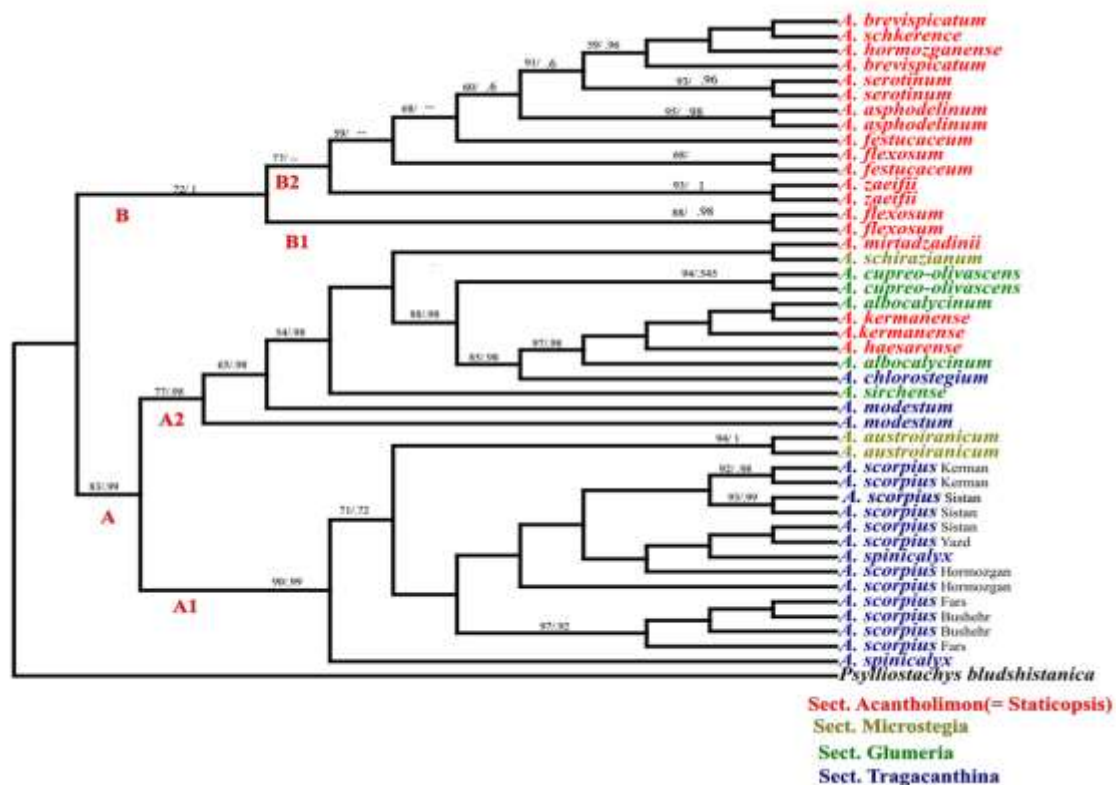


Figure 2. The 50% majority-rule consensus trees were inferred from maximum likelihood analysis using nrDNA ITS sequences. The numbers above the branches represent the maximum likelihood analysis's bootstrap percentage (BP) and posterior probability (PP) of Bayesian inference, respectively.

Results from the rpl32-trnL (UAG) Dataset (Figure 3):

The rpl32-trnL (UAG) matrix also revealed two distinct clades, A and B. The first diverging subclade, A1, included fourteen individuals from the *Tragachantina* section: two accessions of *A. spinicalyx* and twelve of *A. scorpius*. Subclade A2 contained eleven accessions: *A. sarchense* (1; Sect. *Glumeria*), *A. haesarens* (1; Sect. *Acantholimon*), *A. modestum* (2; Sect. *Tragachantina*), *A. kermanense* (1; Sect. *Acantholimon*), *A. chlorostegium* (1; Sect. *Tragachantina*), *A. albocalycinum* (2; Sect. *Glumeria*), *A. austro-iranicum* (2; Sect. *Microstegia*), *A. cupreo-olivascens* (1; Sect. *Glumeria*), and *A. mirtadzinii* (1; Sect. *Acantholimon*). Clade B contained subclades B1 and B2. B1 included one accession of *A. festucaceum* (Sect. *Acantholimon*), while B2 comprised seven *Acantholimon* section accessions: *A. flexosum* (1), *A. serotinum* (1), *A. asphodelinum* (1), *A. zaeifii* (2), and *A. brevispicatum* (2). Phylogenetic analysis employing the combined ITS and rpl32-trnL (UAG) datasets resulted in a tree topology that clearly segregated the sampled accessions into two primary clades, designated Clade A and Clade B (Fig. 4). Clade A further resolved into two well-supported subclades, designated A1 and A2. Subclade A1, representing the basal lineage within Clade A, was composed of sixteen accessions. This group was dominated by taxa from the *Tragachantina* section (*A. spinicalyx* and *A. scorpius*), alongside two accessions identified as *A. austro-iranicum* (Sect. *Microstegia*). Subclade A2 included thirteen accessions distributed across four distinct sections. These accessions comprised: one *A. haesarens* and two *A. kermanense* (Sect. *Acantholimon*); two *A. albocalycinum*, one *A. sarchense*, and two *A. cupreo-olivascens* (Sect. *Glumeria*); one *A. chlorostegium* and two *A. modestum* (Sect. *Tragachantina*); and one *A. shirazianum* (Sect. *Microstegia*). Furthermore, one accession of *A. mirtadzinii* (Sect. *Acantholimon*) was nested within this subclade. Clade B contained subclades B1 and B2. B1 included two accessions of *A. festucaceum* (Sect. *Acantholimon*), while B2 comprised thirteen *Acantholimon* section accessions: *A. flexosum* (3), *A. serotinum* (2), *A. asphodelinum* (2), *A. zaeifii* (2), *A. eschkerense* (1), and *A. brevispicatum* (2).

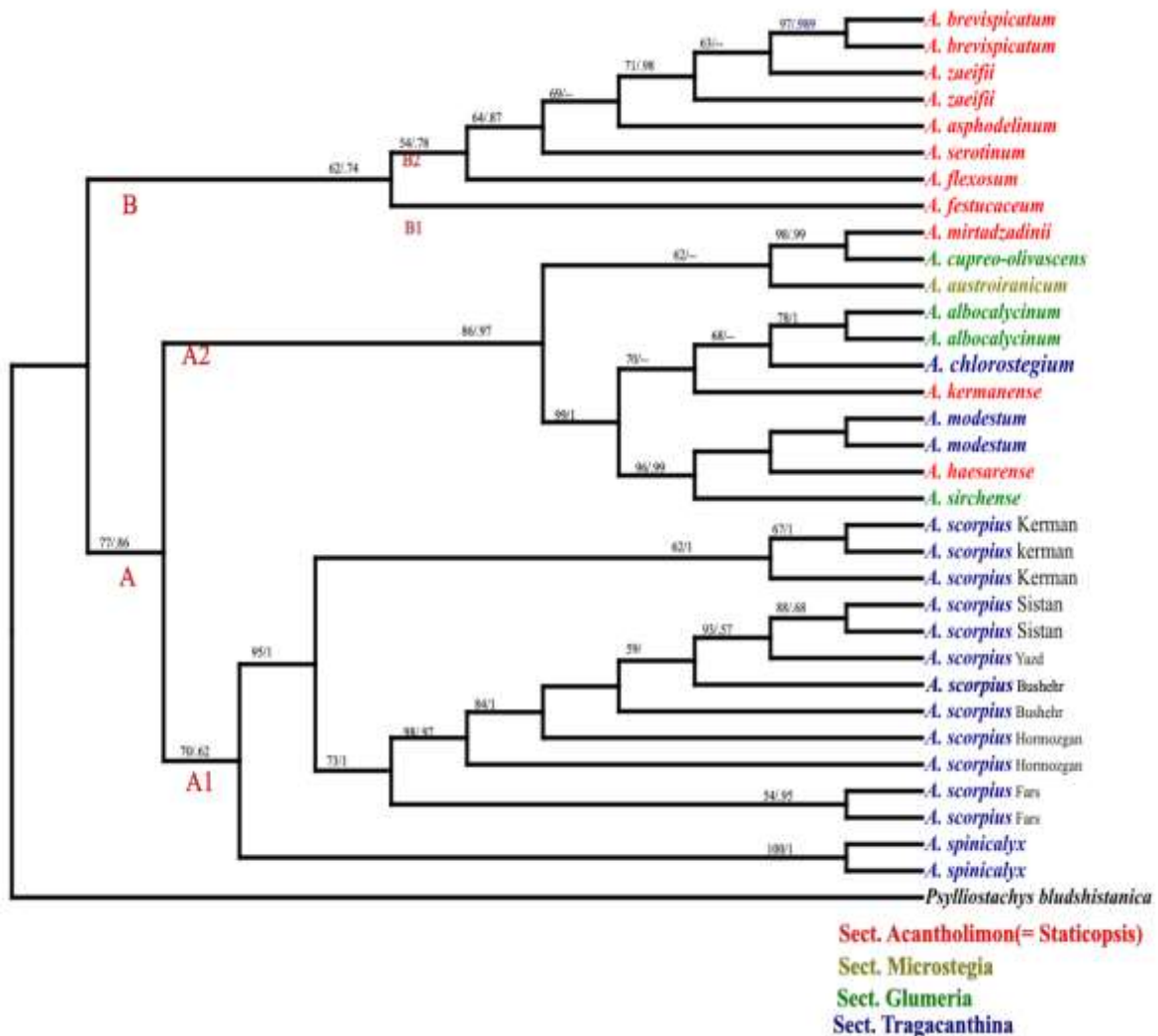


Figure 3. The 50% majority-rule consensus trees were inferred from maximum likelihood analysis using rpl32-trnL (UAG) sequences. The numbers above the branches represent the maximum likelihood analysis's bootstrap percentage (BP) and posterior probability (PP) of Bayesian inference, respectively.



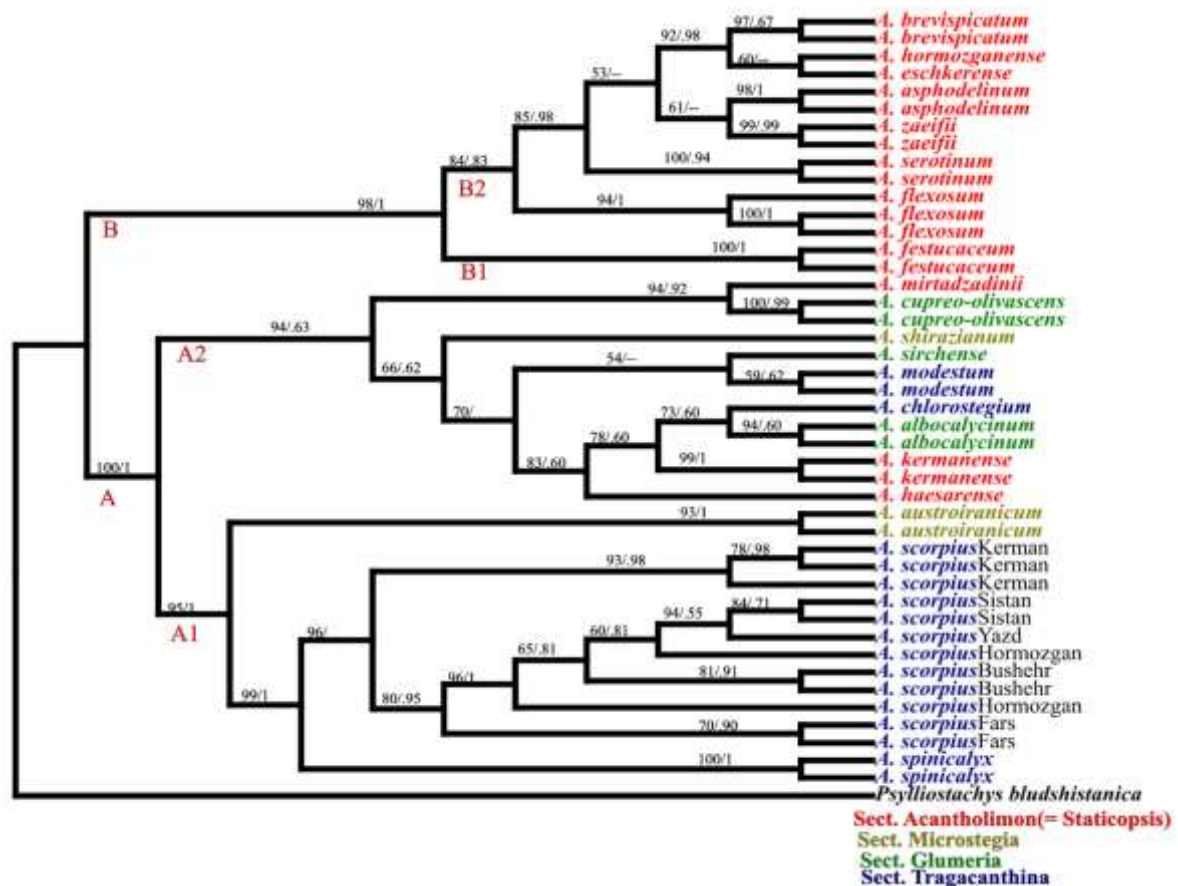


Figure 4. The 50% majority-rule consensus trees were inferred from the combined dataset (nrDNA ITS and rpl32-trnL_(UAG)). The numbers above the branches represent the maximum likelihood analysis's bootstrap percentage (BP) and posterior probability (PP) of Bayesian inference, respectively.

Discussion

The genus *Acantholimon*, with 16 endemic species, exhibits a remarkably high degree of endemism in southern Iran, particularly within Kerman Province. This region is characterized by extensive high-altitude areas and is topographically and floristically connected to the southern Zagros Mountains. The abundance of endemic taxa suggests a complex evolutionary history shaped by geographic isolation, microhabitat specialization, and adaptive radiation (Hedge & Wendelbo, 1978). The topology of phylogenetic trees inferred from nrDNA ITS and rpl32-trnL_(UAG) sequences reveals incongruent placement of certain taxa. These incongruities may result from natural processes such as hybridization, introgression, chloroplast capture, and incomplete lineage sorting (Wendel & Doyle, 1998). This study, which employs the chloroplast marker rpl32-trnL_(UAG) in comparison with the nuclear nrDNA ITS region, may provide a clearer depiction of species relationships. This could be attributed to its higher sequence variability, as indicated by 67 parsimony-informative sites versus 53 in the ITS loci. Moreover, the chloroplast genome is maternally inherited and exhibits a relatively conserved structure. The uniparental mode of chloroplast inheritance tends to minimize the complications associated with hybridization events, which are more frequent in biparentally inherited nuclear genomes, thereby potentially yielding clearer lineage patterns. Nevertheless, integrating data from both nrDNA and cpDNA markers generally provides a more robust and comprehensive phylogenetic resolution. The results of this study, together with those of Moharrek et al. (2017), indicate that the sections *Acantholimon* (= *Staticopsis*), *Glumeria*, *Microstegia*, and *Tragacanthina* do not form monophyletic groups (Figures 2–4). The section *Acantholimon* (= *Staticopsis*) represents the most species-rich group within this genus in Southern Iran, comprising 11 species. Molecular analyses suggest that the species belonging to this section are resolved into two distinct clades within the phylogenetic trees (Figures 2–4). Morphological evidence divides the Southern Iranian *Acantholimon* species into two corresponding groups. Group 1, characterized by a densely arranged terminal spike and multi-flowered spikelets possessing more than two bracteoles, encompasses *A. mirtadzadini*, *A. assadii*, and *A. kermanense*. Group 2 exhibits either dense or lax spikes and features single-flowered, two-bracteolate spikelets, comprising *A. hormozganense*, *A. serotinum*, *A. eschkerense*, *A. asphodelinum*, *A. flexosum*, *A. festucaceum*, *A. zaeifii*, *A. haesarense*, and *A. brevispicatum*. Molecular analyses reveal that Group 1 species are nested within subclade A2, alongside species from other sections. Conversely, Group 2 resides entirely within clade B, with the notable exception of *A. haesarense* (which is also placed in subclade A2). This partitioning demonstrates a high degree of concordance between the morphological and molecular classifications within this section; however, it must be noted that no molecular data are available for *A. assadii* (Figures 2, 4). Three species of the *Glumeria* section (*A. sirschense*, *A. albocalycinum*, and *A. cupreo-olivascens*) are resolved into three distinct positions within subclade A2 (Figures 2–4). This section is morphologically characterized by lax spikes, single or multi-flowered spikelets possessing more than two bracteoles, and spikelets that are consistently

shorter than the nodes. All species within subclade A2 are endemic to Kerman Province, with the exception of *A. shirazianum*. Furthermore, these species largely inhabit restricted mountainous areas and exhibit overlapping geographical distributions, suggesting the formation of a distinct phylogeographical cluster. Despite their molecular proximity, clear morphological distinctions are observed among them. The *Microstegia* section comprises two species: *A. austroiranicum* and *A. shirazianum*, which are allocated to subclades A1 and A2, respectively. The key morphological characteristics defining this section include heteromorphic leaves, dense spikelets containing one to four (1–4) flowers, and a conspicuously pilose, infundibular calyx. *A. austroiranicum* exhibits a close phylogenetic affinity with *A. scorpius*, as evidenced by their similar geographical distribution across southern Kerman, potentially indicating the formation of a distinct phylogeographical cluster. The species *A. scorpius*, *A. spinicalyx*, *A. modestum*, and *A. chlorostegium* belong to the section *Tragacanthina*, which is resolved into three distinct positions across subclades A1 and A2 in the phylogenetic analysis (Figures 2, 3, 4). Common morphological traits shared by these species include heteromorphic leaves, deciduous vernal leaves, lax or dense spikes, and spikelets that are single-flowered and two-bracteate. *A. scorpius* (Jaubert & Spach) Boissier is an endemic species widely distributed throughout Iran, extending into the transitional zone between the Irano-Turanian (IT) and Saharo-Sindian regions (Assadi, 2006). According to the nrDNA ITS tree (Figure 2), individuals of *A. scorpius* populations cluster into a single subclade, adjacent to two individuals of *A. spinicalyx*, despite observed morphological variation in characters such as calyx size, calyx limb structure, calyx vein patterns, and bracteole shape. The co-occurrence of one *A. spinicalyx* individual within the *A. scorpius* population (subclade A1) suggests a close phylogenetic relationship or potential hybridization, necessitating further molecular investigation. While *A. spinicalyx* is characterized by a colored calyx, in contrast to the white calyx of *A. scorpius*, the two species are nevertheless separated based on chloroplast and combined phylogenetic analyses (Figs. 2, 3s). Except for clade B, establishing consistent morphological characters that clearly correspond to the molecular topology of *Acantholimon* species distributed in southern Iran remains difficult. The morphological diversity observed among these species does not consistently reflect their phylogenetic relationships as inferred from molecular data. This incongruence indicates that classical taxonomy, which relies primarily on morphological traits such as leaf indumentum, calyx structure, and spike arrangement, has limited compatibility with molecular phylogenetic evidence. The lack of clear diagnostic morphological features across most clades suggests that convergent evolution or ecological adaptation may obscure phylogenetic signals within the genus. Therefore, integrating molecular markers with detailed morphometric and ecological analyses will be essential to achieve a more reliable systematic framework for *Acantholimon* in southern Iran. Although species of the genus *Acantholimon* are less susceptible to overgrazing because their leaves are rigid and woody, the primary conservation threats stem from habitat destruction due to the expansion of mining activities and the construction of access roads in mountainous areas. These disturbances are critically important for narrowly distributed endemic species in southern Iran, such as *A. shirazianum*, *A. brevispicatum*, *A. hormozganense*, *A. haesarensis*, *A. saadii*, *A. assadii*, *A. mirtadzhadinii*, *A. sarchense*, and *A. cupreo-olivascens*. The combination of small population sizes and restricted ranges renders these specific taxa particularly vulnerable to ongoing habitat fragmentation and anthropogenic disturbance.

Diagnostic Key to the *Acantholimon* species in Southern Iran

1. Inside the calyx pilose..... 2
1. Inside the calyx glabrous 3
2. Spikes terminal, exceeding the leaves; spikelets 2–5; bracteoles oblong..... *A. austroiranicum*
2. Spikes terminal, not exceeding the leaves; spikelets 5–9; bracteoles oblanceolate *A. shirazianum*
3. Spikelets 1-flowered, 2-bracteate 4
3. Spikelets 1- or many-flowered, more than 2-bracteate 16
4. Lower leaves persistent, monomorphic, or broader than upper leaves..... 5
- 4- Lower leaves deciduous, heteromorphic (broader and shorter than upper leaves) 12
5. Calyx white, veins colored 6
5. Calyx colored, veins colored *A. serotinum*
6. Spikes unbranched 7
6. Spikes branched 8
7. Stems short (15–20 mm), not exceeding the leaves; spike short (5–10 mm); bracteoles ovate; petals oblong..... *A. brevispicatum*
7. Stems longer (30–45 mm), exceeding the leaves; spike longer (15–25 mm); bracteoles elliptic; petals spatulate..... *A. zaeifii*
8. Spikes very dense, spikelets imbricate; bracts and bracteoles purple 9
8. Spikes lax, spikelets not imbricate; bracts and bracteoles brown *A. hormozganense*
9. Spikes racemose 10
9. Spikes terminal *A. haesarensis*
10. Spikelets predominantly terminal, occasionally on lateral branches..... *A. asphodelinum*
10. Spikelets predominantly on lateral branches..... 11
11. Spikes with long lateral branches; spikelets lax, bracteoles with long apiculate *A. festucaceum*
11. Spikes with short lateral branches; spikelets dense, bracteoles with short apiculate or obtuse *A. flexuosum*
12. Spikes dense, axis not zigzag; calyx infundibular 13
12. Spikes lax, axis zigzag; calyx tubular *A. saadii*
13. Calyx white 14
13. Calyx colored *A. spinicalyx*
14. Spikelets shorter than 9 mm; calyx shorter than 9 mm..... 15
14. Spikelets longer than 9 mm; calyx longer than 8 mm *A. scorpius*
15. Spikes lax; calyx milky white; calyx veins not reaching tips of lobes *A. chlorostegium*
15. Spikes dense; calyx white to brown; calyx veins reaching tips of lobes *A. modestum*
16. Spikes terminal; spikelets longer than internodes 17



16. Spikes not terminal; spikelets shorter than internodes 19
 17. Spikes dense; calyx light to dark brown *A. assadii*
 17. Spikes terminal; calyx purple 18
 18. Spikes exceeding or nearly the leaves; leaves 2 mm in width; bracteoles apiculate *A. mirtadzinii*
 18. Spikes exceeding or very much longer than leaves; leaves 1 mm in width; bracteoles obtuse *A. kermanense*
 19. Calyx white *A. albocalycinum*
 19. Calyx purple or brown 20
 20. Bracts lanceolate, reaching to the middle or two-thirds of bracteoles *A. sirchense*
 20. Bracts ovate, reaching up to one-third of bracteoles *A. cupreo-olivascens*

Acknowledgements

The authors thank the Herbarium for their support of the Research Institute of Forests and Rangelands (TARI) for their cooperation. This work was funded by the Tarbiat Modares University Research Council.

References

- Assadi, M. (2004). Two new species of the genus *Acantholimon* Boiss. (Plumbaginaceae) from Iran. *The Iranian Journal of Botany*, 10(1), 25–29. https://ijb.areeo.ac.ir/article_103506.html
- Assadi, M. (2005a). Plumbaginaceae Juss. In M. Asadi & A. A. Maassumi (eds.) *Flora of Iran* (Vol 51). Research Institute of Forests and Rangelands Publications. [In Persian]
- Assadi, M. (2005b). Four new species of the genus *Acantholimon* Boiss. (Plumbaginaceae) From Iran. *The Iranian Journal of Botany*, 11(1), 31–39. https://ijb.areeo.ac.ir/article_102860.html
- Assadi, M. (2006). Distribution patterns of the genus *Acantholimon* (Plumbaginaceae) in Iran. *The Iranian Journal of Botany*, 12(2), 114–120. https://ijb.areeo.ac.ir/article_102790.html
- Assadi, M., & Mirtadzinii, S. M. (2006). Three new species of *Acantholimon* (Plumbaginaceae) from Iran. *The Iranian Journal of Botany*, 11(2), 129–136. https://ijb.areeo.ac.ir/article_102876.html
- Assadi, M., & Zeraatkar, A. (2020). *Acantholimon saadii* (Plumbaginaceae), a new species from Iran. *The Iranian Journal of Botany*, 26(1), 1–5. <https://doi.org/10.22092/ijb.2020.342569.1277>
- Bibak, H., Kazempour-Osaloo, S., & Assadi, M. (2024). *Acantholimon brevispicatum* (Plumbaginaceae), a New Species from South-eastern Iran Based on Morphological and Molecular Data. *Iranian Journal of Science*, 49, 11–19. <https://doi.org/10.1007/s40995-024-01688-8>
- Bordbar, F., & Mirtadzinii, S. M. (2022). *Acantholimon assadii* (Plumbaginaceae), a new species from the flora of Iran. *Phytotaxa*, 574(1), 99–104. <https://doi.org/10.11646/phytotaxa.574.1.7>
- Douzery, E., Pridgeon, A., Kores, P., Linder, H. P., Kurzweil, H., & Chase, M. (1999). Molecular phylogenetics of *Diseae* (Orchidaceae): a contribution from nuclear ribosomal ITS sequences. *American Journal of Botany*, 86(6), 887–899. <https://doi.org/10.2307/2656709>
- Doyle, J. J., & Doyle, J. L. (1987). A rapid DNA isolation of fresh leaf tissue. *Phytochem, Bull*, 19, 11–5. <https://doi.org/10.4236/oji.2013.34028>
- Ghahremaninejad, F., Alirezai, Z., Mohammadi, M., & Nejad Falatoury, A. (2025). Updated catalogue of Iran's endemic angiosperms. *Taxonomy and Biosystematics*, 17(3), 23–70. <https://doi.org/10.22108/tbj.2025.146441.1314>
- Hassler, M. (2004–2023). *World Plants. Synonymic Checklist and Distribution of the World Flora*. Version 16.4. Available from <https://B2n.ir/df7873> (Accessed: 22 September 2023).
- Hedge, I. C. & Wendelbo, P. (1978). Patterns of distribution and endemism in Iran. *Notes from the Royal Botanic Garden Edinburgh*, 36(2), 441–464. <https://journals.rbge.org.uk/notes/article/download/3130/2950>
- Khajoei-Nasab, F., & Khosravi, A.R. (2020). Identification of the areas of endemism (AOEs) of the genus *Acantholimon* (Plumbaginaceae) in Iran. *Plant Biosystems*, 154(5), 726–736. <https://doi.org/10.1080/11263504.2019.1686078>
- Kubitzki, K. (1993). Plumbaginaceae. In K. Kubitzki, J.G. Rohwer & V. Bittrich (eds.), *The families and genera of vascular plants* (Vol 2; pp. 523–530). Springer. https://doi.org/10.1007/978-3-662-02899-5_62
- Mahmoodi, M., & Assadi, M. (2021). A new species of *Acantholimon* (Plumbaginaceae) from Iran. *The Iranian Journal of Botany*, 27(2), 71–77. <https://doi.org/10.22092/ijb.2021.356512.1341>
- Miller, M. A., Pfeiffer, W., & Schwartz, T. (2010, November). Creating the CIPRES Science Gateway for inference of large phylogenetic trees. In *2010 gateway computing environments workshop (GCE)* (pp. 1–8). Ieee. <https://doi.org/10.1109/GCE.2010.5676129>
- Mobayen, S. (1964). *Révision taxonomique du genre Acantholimon*. Tehran.



- Moharrek, F., Kazempour Osaloo, S. H., & Assadi, M. (2014). Molecular phylogeny of Plumbaginaceae with emphasis on *Acantholimon* Boiss. Based on nuclear and plastid DNA sequences in Iran. *Biochemical Systematics and Ecology*, 57, 117-127. <https://doi.org/10.1016/j.bse.2014.07.023>
- Moharrek, F., Kazempour Osaloo, S. H., Assadi, M., & Gonzalo Nieto Feliner. (2017). Molecular phylogenetic evidence for a wide circumscription of a characteristic Irano-Turanian element: *Acantholimon* (Plumbaginaceae: Limonioideae). *Botanical Journal of the Linnean Society*, 184, 366–386. <https://doi.org/10.1093/botlinnean/box033>
- Moharrek, F., Sanmartín, I., Kazempour Osaloo, S.H., & Gonzalo Nieto Feliner. (2019). Morphological Innovations and Vast Extensions of Mountain Habitats Triggered Rapid Diversification Within the Species-Rich Irano-Turanian Genus *Acantholimon* (Plumbaginaceae). *Frontiers in Genetics*, 9, 1-15. <https://doi.org/10.3389/fgene.2018.00698>
- Posada, D. (2008). jModelTest: phylogenetic model averaging. *Molecular biology and evolution*, 25(7), 1253-1256. <https://doi.org/10.1093/molbev/msn083>
- POWO. (2024). *Plants of the World Online*. Facilitated by the Royal Botanic Gardens, Kew. Published on the Internet; <http://www.plantsoftheworldonline.org/> Retrieved 19 March 2024.
- Rechinger, K.H., & Schiman-Czeika, H. (1974). Plumbaginaceae. In K. H. Rechinger, (Ed.) *Flora Iranica* (Vol. 108). Akademische Druck- u. <https://B2n.ir/wb2115>
- Ronquist, F., Teslenko, M., van der Mark, P., Ayres, D. L., & Darling, A. (2012). MrBayes 3.2: Efficient Bayesian phylogenetic inference and model choice across a large model space. *Systematic Biology*, 61(3), 539-542. <https://doi.org/10.1093/sysbio/sys029>
- Sánchez, P., Serra, F., Tárraga, J., Medina, I., & Carbonell. (2011). Phylemon 2.0: a suite of web tools for molecular evolution, phylogenetics, phylogenomics, and hypothesis testing. *Nucleic Acids Research*, 39, 470-474. <https://doi.org/10.1093/nar/gkr408>
- Shaw, J., Lickey, E. B., Schilling, E. E., & Small, R. L. (2007). Comparison of whole chloroplast genome sequences to choose noncoding regions for phylogenetic studies in angiosperms: the tortoise and the hare III. *American Journal of Botany*, 94(3), 275-288. <https://doi.org/10.3732/ajb.94.3.275>
- Trifinopoulos, J., Nguyen, L. T., von Haeseler, A., & Minh, B. Q. (2016). W-IQ-TREE: a fast online phylogenetic tool for maximum likelihood analysis. *Nucleic Acids Research*, 44(W1): W232- W235. <https://doi.org/10.1093/nar/gkw256>
- Wendel, J. F., & Doyle, J. J. (1998). Phylogenetic incongruence: window into genome history and molecular evolution. In P. S. Soltis, D. E. Soltis & J. J. Doyle (eds.), *Molecular Systematics of Plants II* (pp. 265-296), Dordrecht, Kluwer. https://doi.org/10.1007/978-1-4615-5419-6_10

